Respiratory Attractor Dynamics and Their Association with Symptom Burden in COPD

Passara Chanchotisatien, DK Arvind
Speckled Computing
The University of Edinburgh
passara.chanchotisatien@ed.ac.uk, dka@inf.ed.ac.uk

***Abstract*—Chronic obstructive pulmonary disease (COPD) is characterised by persistent respiratory symptoms and activity limitations. While tools like the COPD Assessment Test (CAT) enable self-reported monitoring, they lack physiological objectivity and temporal resolution. This study investigates the use of *phase-space attractor reconstruction*, a nonlinear time-series method, for symptom tracking using respiratory signals from a chest-worn accelerometer. Data from 12 COPD patients over four to six weeks were segmented using a CNN-BiGRU-based activity classifier to isolate stationary periods. *Attractor reconstructions* were computed at 60-second intervals, and 112 features spanning geometric, spectral, and topological domains were extracted. Several features showed noteworthy correlations with total and item-level CAT scores, supporting their potential as objective markers of symptom burden. These results highlight the feasibility of attractor-based analysis for non-invasive, continuous COPD monitoring and personalised disease management.**

***Index Terms*—Chronic obstructive pulmonary disease, Respiratory signal processing, Wearable sensors, Nonlinear signal analysis, Feature extraction, Patient monitoring**

I. Introduction

Chronic obstructive pulmonary disease (COPD) is a progressive condition characterised by airflow limitation and symptoms such as breathlessness, cough, and fatigue [1]. It remains a major global health burden, causing over 3.5 million deaths in 2021, with prevalence expected to rise by 2050 [2]. Tools like the COPD Assessment Test (CAT) [3] enable accessible, patient-centred symptom monitoring, but lack temporal resolution. Wearable sensors offer a promising alternative for continuous, objective respiratory monitoring, yet are challenged by motion artefacts and signal noise. Conventional metrics—such as respiratory rate or amplitude—are scalar summaries that often overlook subtle, time-varying changes in waveform morphology, limiting their sensitivity to early or transient symptom deterioration.

To address these limitations, phase-space attractor reconstruction (AR) [4] has emerged as a nonlinear method for reconstructing time-series data into geometric attractors that capture underlying dynamical properties. In this study, the reconstructed trajectories were projected into two-dimensional space, enabling geometric, spectral, and topological feature extraction following prior implementations [5], [6]. AR enables detailed characterisation of signal morphology and has shown utility in cardiac, respiratory, and behavioural contexts [5], [6]. However, its application to wearable-derived respiratory signals remains unexplored.

This study investigates the utility of AR for continuous symptom monitoring in individuals with COPD, using respiratory data from a chest-worn accelerometer. We examine whether features extracted from attractor structures are associated with daily CAT scores—a validated eight-item questionnaire commonly used by clinicians to assess patient-perceived symptom burden across domains such as breathlessness, cough, sleep, and listlessness [3]. While subjective, the CAT remains a practical benchmark in both research and clinical care [7]. We treat it not as a physiological ground truth, but as a reference to evaluate whether wearable-derived respiratory features can reflect perceived symptom burden. Demonstrating such alignment in this exploratory analysis would support the potential of attractor-based features as candidate digital biomarkers, offering insight into symptom dynamics beyond those captured by episodic assessments alone.

A. Methodology

1) RESpeck Device and Dataset: The RESpeck device [8] is a compact, chest-worn wireless sensor developed at the University of Edinburgh for monitoring respiratory effort. It uses a triaxial accelerometer positioned on the left lower costal margin to capture chest wall motion, sampling at 12.5 Hz and transmitting data via Bluetooth. Reconstructed respiratory waveforms show strong agreement with nasal cannula measurements for flow ($r = 0.9597$) and rate ($r = 0.9848$, RMS error = 0.38 BPM) [9] [10]. Eighteen individuals with COPD were recruited from NHS Borders General Hospital after being prescribed pulmonary rehabilitation. Each wore the RESpeck device continuously for four to six weeks and were encouraged to complete the CAT daily. The CAT is a validated eight-item questionnaire assessing symptom burden, with scores ranging from 0 to 40; higher scores indicate greater disease impact [3].

B. Respiratory Signal Preprocessing

To enable reliable respiratory analysis, stationary periods (sitting, standing, lying down) were identified using a CNN-BiGRU activity classifier trained on accelerometer

This work was supported by the UKRI CDT in Biomedical AI (EP/S02431X/1), the Centre for Speckled Computing, and UKRI grants DAPHNE (NE/P016340/1) and PHILAP (MR/R024405/1). NHS Borders approved the COPD data collection (Ref: 21/BORD/IN01) under the study titled Remote Monitoring and Pulmonary Rehabilitation of COPD Patients in the NHS Borders Region.

data from 152 volunteers, achieving 94% accuracy (95% CI: 0.935–0.948) via 10-fold cross-validation [11]. Sensor data were segmented into 60-second windows, discarding windows with motion, missing values, or prone/left-facing posture due to sensor placement. Incomplete or short segments were excluded.

C. Attractor Reconstruction and 2D Projection

Phase-space attractor reconstruction [5] embeds approximately periodic respiratory signals into a two-dimensional space that captures waveform morphology. Given a signal $x(t)$, an N-dimensional delay embedding is formed as:

$$\mathbf{x}_N(t) = [x(t),\, x(t-\tau),\, \ldots,\, x(t-(N-1)\tau)]^T \in \mathbb{R}^N \quad (1)$$

The delay vectors are projected onto an orthonormal basis, yielding two-dimensional coordinates $(a_{N,k}(t), b_{N,k}(t))$ [5]:

$$a_{N,k}(t) = \tfrac{1}{\sqrt{N}} \sum_{j=0}^{N-1} \cos\Big(\tfrac{2\pi jk}{N}\Big)\, x(t-j\tau), \quad (2)$$

$$b_{N,k}(t) = -\tfrac{1}{\sqrt{N}} \sum_{j=0}^{N-1} \sin\Big(\tfrac{2\pi jk}{N}\Big)\, x(t-j\tau), \quad (3)$$

for $k = 1, \ldots, \lfloor (N-1)/2 \rfloor$. The resulting trajectory forms a two-dimensional, shift-invariant attractor that encodes waveform structure. In this study, the delay parameter τ was estimated using mutual information and autocorrelation methods [12]–[14], converging on $\tau = 9$ samples. Reconstructions were generated with embedding dimension $N = 3$ and projection index $k = 1$, producing one two-dimensional attractor per 60-second respiratory window (Figure 1a).

D. Feature Extraction

To characterise the structure and dynamics of attractors derived from respiratory signals, we extracted 34 features spanning statistical, geometric, spectral, complexity, and recurrence domains. Attractors were constructed by projecting delay-embedded respiratory signals into two dimensions, (a_k, b_k) as described in Section I-C. Features were primarily computed from the raw projections to preserve scale and distribution, except for Recurrence Quantification Analysis (RQA), where projections were standardised (zero mean, unit variance) to ensure consistent thresholding across windows.

1) ***Statistical Features****:* Distributional properties of a_k and b_k were summarised using variance (VAR A, VAR B), skewness (SKEW A, SKEW B), and kurtosis (KUR A, KUR B) for each attractor axis. The Pearson correlation coefficient between axes (COR) captured linear dependency, while the coefficient of variation (COV A, COV B) on each axis provided a scale-normalised measure of variability.

2) ***Geometric Features****:* Spatial structure was quantified using convex hull area (CHA), aspect ratio (AR; ratio of axis ranges), and radius of gyration (Rg; RMS distance to centroid). Attractor compactness (AC), the ratio of standard deviation to mean centroid distance, captured clustering. Additional metrics included eccentricity (ECC; square root of PCA eigenvalue ratio), attractor diameter (AD; maximum pairwise distance), and mean centroid distance (MCD).

3) ***Recurrence Quantification Analysis (RQA)****:* Temporal structure was assessed via RQA [15]. Recurrence plots were computed by thresholding pairwise distances between standardised attractor points using a fixed distance percentile. Extracted metrics included recurrence rate (RR), determinism (DET), laminarity (LAM), trapping time (TT), average diagonal line length (ADL), and recurrence entropy (RE).

4) ***Spectral Features****:* Spectral characteristics were extracted from the power spectral density of each axis and included spectral mean (PSDM A and PSDM B), peak frequency (PSDP A and PSDP B), peak-to-peak amplitude (PTP A and PTP B), and zero-crossing rate (ZCR A and ZCR B).

5) ***Complexity Features****:* Complexity was captured across spatial, fractal, dynamical, and topological dimensions. Joint entropy (JE) was computed from a 2D histogram with adaptive binning to quantify spatial dispersion. Fractal structure was measured via box-counting dimension. Dynamical complexity was assessed using the largest Lyapunov exponent (LLE), reflecting sensitivity to initial conditions. Topological complexity was estimated using graph entropy (GE), calculated from the Shannon entropy of degree distributions in a k-nearest neighbour graph.

E. Analysis

The relevance of attractor-derived features to COPD symptoms was assessed using daily feature summaries. For each subject and each day, the 34 features were aggregated by computing the mean (μ), standard deviation (σ), minimum (min), and maximum (max), yielding 136 daily summary features. Spearman rank correlations were then computed between aggregated feature values and CAT scores, with each CAT entry paired to the preceding 24 hours of RESpeck data, for subjects with at least 10 CAT entries ($n = 12$). Associations with $|\rho| \geq 0.3$ and $p < 0.05$ were deemed noteworthy. Both total and item-level CAT scores were analysed; for CAT Q7 (sleep), analysis was restricted to respiratory data recorded in the supine or right-facing position. Table I provides the number of data windows (in hours), CAT entries, and average CAT score (with standard deviation) for each subject.

II. Results and Discussion

Figure 1 shows visualisations of attractor morphology features and its relationship to symptom burden. Panel (b) presents representative attractors across quantile bins for two features (DET and Rg), illustrating how geometry varies with magnitude, revealing morphological trends with increasing feature magnitude—e.g., higher DET values correspond to

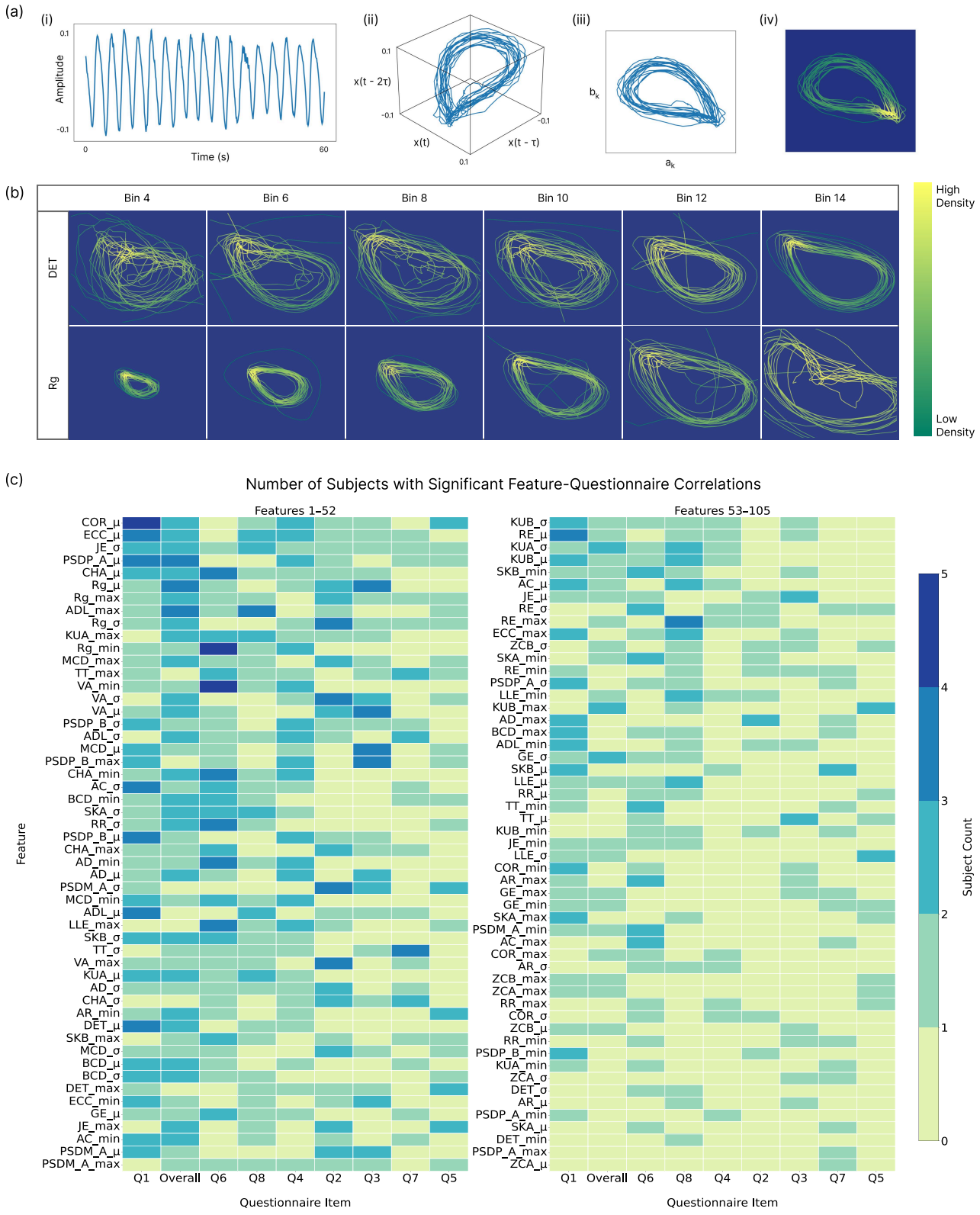

Fig. 1. *Attractor morphology and CAT score associations.* (a) Illustration of delay embedding and attractor reconstruction and 2D projection of a breathing signal. (b) Example attractors grouped into 15 quantile-based bins for two different features. Each column represents a bin containing attractors whose feature values fall within a specific percentile range. Columns are ordered left to right by increasing feature magnitude. Attractors are overlaid using density contours (yellow: high density; green: low density) to highlight regions of repeated phase-space visitation across windows. (c) Heatmap showing the number of subjects ($n \leq 12$) with noteworthy correlations ($|\rho| \geq 0.3$, $p < 0.05$) between attractor-derived features and CAT items (Q1–Q8) or total score. Features are grouped into two panels and labelled as *feature_axis_statistic* (daily mean, STD, min, or max). Darker shades indicate greater cross-subject relevance. Rows and columns are sorted by the total number of subjects and features, respectively, with significant associations.

TABLE I
SUMMARY OF CAT SCORES AND DATA COUNT PER SUBJECT

Subject ID	Num windows (hrs)	Num CAT Scores	Average CAT Score (STD)
PRB003	15.4k (≈256.31 hrs)	17	6.18 (1.38)
PRB006	15.5k (≈257.82 hrs)	13	23.46 (2.90)
PRB007	14.4k (≈239.3 hrs)	19	17.16 (2.03)
PRB103	31.7k (≈528.6 hrs)	33	5.72 (1.44)
PRB105	22.4k (≈373.45 hrs)	44	13.73 (2.13)
PRB107	9.7k (≈161.92 hrs)	45	13.13 (6.01)
PRB108	32.92k (≈548.71 hrs)	26	8.42 (2.30)
PRB201	22.84k (≈380.68 hrs)	94	23.06 (2.40)
PRB202	17.28k ≈288.05 hrs)	44	16.86 (7.11)
PRB203	27.48k (≈458.01 hrs)	52	22.44 (2.43)
PRX018	39.15k (≈652.43 hrs)	26	18.77 (1.37)
PRX900	25.5k (≈425.03 hrs)	43	12.23 (3.54)

more coherent, looped structures, consistent with more predictable respiratory dynamics [6]. Rg quantifies the average distance of points from the centroid, capturing overall dispersion. Panel (c) summarises the number of subjects with significant correlations ($|\rho| \geq 0.3$, $p < 0.05$) between attractor-derived features and CAT items or total score. The heatmap highlights features that consistently reflect symptom variation and sensitivity to specific CAT questions.

In Panel (c), the features most frequently exhibiting significant correlations with CAT items across subjects included COR_μ, ECC_μ, JE_σ, $PSDP\_A\_\mu$, and Rg_μ. These features primarily capture geometric and spectral properties of attractors, such as axis correlation, eccentricity, and spatial dispersion, and demonstrate consistent associations across multiple questionnaire items and subjects. Among the CAT items, Q1 (cough) showed the highest number of significant feature associations (117), followed by the total CAT score (101), Q6 (confidence leaving home) (100), Q8 (energy levels) (77), and Q4 (breathlessness) (63). This distribution suggests that attractor-derived features are particularly sensitive to symptoms related to physical discomfort, exertional confidence, and fatigue. Several attractor-derived features computed as daily minima or maxima were significantly correlated with CAT scores, underscoring the relevance of extreme respiratory behaviours to perceived symptom burden. These findings support the idea that minimum and maximum features offer sensitivity to transient or episodic physiological deviations that are not captured by average metrics, yet are nonetheless salient in the patient's daily symptom perception.

III. CONCLUSION

This research demonstrates the feasibility of using attractor-derived features collected from chest-worn sensor data to track COPD symptom burden. By extracting attractor-based metrics during stationary periods and correlating them with self-reported CAT scores, we identified consistent associations between geometric, spectral, and variability-based features and specific symptom domains. Attractor-derived features such as radius of gyration and recurrence entropy showed robust correlations with self-reported symptom severity according to the CAT score. Although the sample size was limited ($n = 12$), each participant contributed a substantial volume of data, averaging 380.86 hours of continuous respiratory data. This rich, longitudinal dataset strengthens the validity of the findings despite the small cohort. The results offer promising evidence for the integration of attractor-derived into wearable-based COPD monitoring. Future work will focus on larger cohorts and predictive modelling to assess the utility of attractor-derived features for early detection of symptom deterioration and exacerbation risk.

REFERENCES

[1] N. Al Wachami, M. Guennouni, Y. Iderdar, K. Boumendil, M. Arraji, Y. Mourajid, F. Z. Bouchachi, M. Barkaoui, M. L. Louerdi, A. Hilali *et al.*, "Estimating the global prevalence of chronic obstructive pulmonary disease (copd): a systematic review and meta-analysis," *BMC Public Health*, vol. 24, no. 1, p. 297, 2024.

[2] World Health Organization, "Chronic obstructive pulmonary disease (copd)," 2023, accessed: 2025-05-11. [Online]. Available: https://www.who.int/news-room/fact-sheets/detail/chronic-obstructive-pulmonary-disease-(copd)

[3] P. Jones, G. Harding, P. Berry, I. Wiklund, W. Chen, and N. K. Leidy, "Development and first validation of the copd assessment test," *European Respiratory Journal*, vol. 34, no. 3, pp. 648–654, 2009.

[4] M. Nandi and P. J. Aston, "Extracting new information from old waveforms: Symmetric projection attractor reconstruction: Where maths meets medicine," *Experimental physiology*, vol. 105, no. 9, pp. 1444–1451, 2020.

[5] J. Lyle and P. Aston, "Symmetric projection attractor reconstruction: Embedding in higher dimensions," *Chaos: An Interdisciplinary Journal of Nonlinear Science*, vol. 31, no. 11, 2021.

[6] M. Serna-Pascual, R. F. D'Cruz, M. Volovaya, C. J. Jolley, N. Hart, G. F. Rafferty, J. Steier, P. J. Aston, and M. Nandi, "Novel breathing pattern analysis: Symmetric projection attractor reconstruction improves identification of impending copd re-exacerbations–a retrospective cohort analysis," *ERJ Open Research*, vol. 9, no. 4, pp. 00 164–2023, 2023.

[7] T. Glaab, C. Vogelmeier, and R. Buhl, "Outcome measures in chronic obstructive pulmonary disease (copd): strengths and limitations," *Respiratory research*, vol. 11, pp. 1–11, 2010.

[8] D. Arvind, D. Fischer, C. Bates, and S. Kinra, "Characterisation of breathing and physical activity patterns in the general population using the wearable respeck monitor," in *Body Area Networks: Smart IoT and Big Data for Intelligent Health Management: 14th EAI International Conference, BODYNETS 2019, Florence, Italy, October 2-3, 2019, Proceedings 14*. Springer, 2019, pp. 68–78.

[9] A. Bates, M. J. Ling, J. Mann, and D. Arvind, "Respiratory rate and flow waveform estimation from tri-axial accelerometer data," in *2010 International Conference on Body Sensor Networks*, 2010, pp. 144–150.

[10] G. B. Drummond, D. Fischer, M. Lees, A. Bates, J. Mann, and D. Arvind, "Classifying signals from a wearable accelerometer device to measure respiratory rate," *ERJ Open Research*, vol. 7, no. 2, 2021.

[11] P. Chanchotisatien and D. K. Arvind, "Coughing in steps: Transferring knowledge from dynamic physical activity dataset to respiratory disturbance classification," in *Proceedings of the 20th IEEE International Symposium on Medical Measurements and Applications (MeMeA)*. IEEE, Feb. 2025.

[12] A. M. Fraser and H. L. Swinney, "Independent coordinates for strange attractors from mutual information," *Physical review A*, vol. 33, no. 2, p. 1134, 1986.

[13] S. Wallot and D. Mønster, "Calculation of average mutual information (ami) and false-nearest neighbors (fnn) for the estimation of embedding parameters of multidimensional time series in matlab," *Frontiers in psychology*, vol. 9, p. 1679, 2018.

[14] S. P. Garcia and J. S. Almeida, "Nearest neighbor embedding with different time delays," *Physical Review E—Statistical, Nonlinear, and Soft Matter Physics*, vol. 71, no. 3, p. 037204, 2005.

[15] C. L. Webber and N. Marwan, "Recurrence quantification analysis," *Theory and best practices*, vol. 426, 2015.